Image-based Finite-Element Bone Mechanics Simulations: Does Stiffness Predict Yield Strength?

Ning Zhang[1], Jeremy Magland[1], Chamith Rajapakse[1], Yusuf Bhagat[1], and Felix Wehrli[1]

[1]*Department of Radiology, University of Pennsylvania, Philadelphia, PA, United States*

Introduction:

High-resolution MR or CT image-based micro-finite element (μFE) modeling has shown promise for estimating bone mechanical behavior and assessing osteoporotic fracture risk [1]. Other applications of interest involve assessment of the response to drug intervention on bone mechanical competence [2]. However, limitations in computing power of desktop systems practically have limited μFE models to the linear regime yielding elastic constants such as compressive and shear moduli. In contrast, nonlinear μFE models are capable of predicting bone's failure strength. Unfortunately, nonlinear μFE modeling is computationally far more demanding, increasing computation times by one to two orders of magnitude. The purpose of this work was to apply a recently developed efficient algorithm [3] to μFE analysis in the nonlinear regime. Specifically, we were interested in exploring the relationship between trabecular bone (TB) yield stress predicted by nonlinear μFE models and the axial stiffness computed from linear μFE models. A few studies have reported correlations between these two quantities using either μCT-based μFE simulation of bovine tibial specimens [4] or mechanical testing results on specimens from four clinically relevant sites [5]. Here, we present initial results on the basis of μCT images of human distal tibia specimens as well as *in-vivo* μMR images of the distal tibia of selected subjects from an ongoing clinical study at 7T.

Methods:

Image acquisition and processing: μCT images at 25 μm isotropic voxel size of the human distal tibia from 10 donors were selected to cover a range of axial stiffness values. Whole bone regions (cortical and TB) were first segmented and the resultant binarized images downsampled to low-resolution images at 100 μm isotropic voxel size, comparable to *in-vivo* μMR images. Further, *in-vivo* μMR images of the distal tibia of ten postmenopausal women were previously acquired with a 3D fast spin echo with out-of-slab cancellation (FSE-OSC) sequence [6] at 137 x 137 x 410 μm^3 voxel size on a Siemens 7T whole-body system. All images were first manually masked to isolate the TB region, and then sinc-interpolated along the longitudinal direction resulting in images with isotropic voxel size. Subsequently, the resultant images were normalized and inverted to generate the grayscale bone volume fraction (BVF) maps [7] as input to both the linear and nonlinear μFE models.

Linear μFE modeling: Axial stiffness was calculated by linear μFE analysis using a custom-designed program [3] where bone tissue was assumed linear elastic under small strains. Thus, a linear system was established and solved for the resultant displacements and the primary stress using a preconditioned conjugate gradient method. Boundary conditions were set to represent axial compression with no friction along the transverse directions. A small strain (0.1%) in the axial direction was applied to nodes at the top surface while nodes at the bottom surface were fixed. Nodes at both the top and bottom surfaces were free to move in the transverse plane. Axial stiffness was then obtained as the primary stress over the applied strain.

Nonlinear μFE modeling: Yield stress was predicted by nonlinear μFE analysis with a two-step procedure. The first step was to obtain a stress-strain curve, which is the best fit to a series of points of gradually applied incremental strains and their corresponding stresses. At very small strains the linear μFE model was used to obtain the corresponding stresses. At increasing strains, however, trabecular tissue exhibits nonlinear stress-strain behavior. In our approach, trabecular tissue was assumed to be regionally linear elastic. However, as tissue compressive strain approaches yield strain, tissue post-yield modulus was reduced to 80% of its original value; when tissue compressive strain exceeded yield strain by less than 200%, tissue post-yield modulus was reduced by 70%. Further, when tissue compressive strain exceeded yield strain by 200%, tissue post-yield modulus was reduced to 5%. The boundary conditions were the same as in the linear model to simulate axial compression tests. The nonlinear system was then solved for the corresponding stress using Newton's method. The second step was to fit the stress-strain curve to these points of applied strains and corresponding stresses with cubic polynomials. Lastly, the apparent yield stress and strain were obtained based on the 0.2% offset rule [4].

Results and Discussion:

The μCT and μMR image-based μFE models contained 2.9 ± 1.0 and 0.5 ± 0.1 million elements, respectively. Nonlinear simulations required 18.1 ± 7.5 hours for the μCT data and 5.6 ± 2.7 hours for the μMR data, respectively, on a desktop computer with four dual processors i7-2600 3.40 GHz CPUs and 8 GB of RAM. Nine strain levels with a minimum increment of 0.1% were applied to obtain each curve. Fig. 1a shows a plot of a typical stress-strain curve from nonlinear μFE simulation on the basis of a μMR image data set (Fig. 1b). The mean ($\pm$SD) of BV/TV, the estimated axial stiffness, the derived yield stresses and strains were $7.82 \pm 1.36\%$, 320.26 ± 76.10MPa, 1.81 ± 0.56 MPa and $0.79 \pm 0.04\%$, respectively, for the μMR data, and $22.73 \pm 6.16\%$, 1.56 ± 0.57 GPa, 10.73 ± 3.30 MPa and $0.89 \pm 0.03\%$, respectively, for the μCT data. The inclusion of cortical bone in the *ex-vivo* data led to a much larger BVF, and thus axial stiffness and yield stress compared to those of the *in-vivo* data. At the yield point, $2.02 \pm 0.46\%$ of the bone tissue volume was strained beyond the tissue yield strain for the μMR data and $1.96 \pm 0.42\%$ for the μCT data. These results are consistent with previous reports [5,8]. Simulated strain maps (Figs. 1c-f) from applying different amounts of strains (0.1%, 0.4%, 0.7% and 0.9%) are also given showing some trabeculae were increasingly strained until failure occurred. Figs. 1g and h compare yield stress and axial stiffness from nonlinear and linear analysis, respectively (μMR (g), μCT (h)). Strong correlation between these two parameters were found for both μCT and μMR images suggesting that the axial stiffness derived from linear μFE analysis may be able to predict trabecular bone's yield stress.

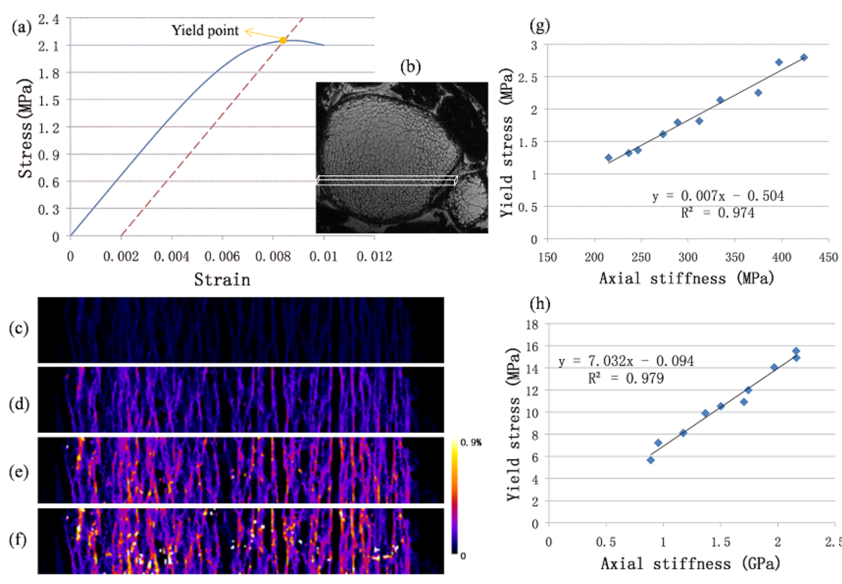

Fig. 1. Example of μMRI-derived simulated stress-strain curve (a) based on a 3D image data set (b); longitudinal projections of simulated strain maps of a thin slab indicated in (b) for different levels of applied strain (0.1% (c), 0.4% (d), 0.7% (e) and 0.9% (f)); correlations between axial stiffness from linear simulations and yield stress predicted from nonlinear simulations based on μMR (g) and μCT images (h).

References: [1] Boutroy, JBMR, 23:392-99, (2008); [2] Wehrli, JBMR, 25:1406-14, (2010); [3] Zhang, proc. ISMRM, (2011); [4] Niebur, J Biomech, 33:1575-83, (2000); [5] Morgan, J Biomech, 34:569-77, (2001); [6] Magland, MRM, 63(3):719, (2010); [7] Rajapakse, Bone, 47:556-63, (2010); [8] Pistoia, Bone, 30(6):842-48, (2002). **Acknowledgement:** NIH grants R01 AR55647 and RO1 AR53156.